AIMS Materials Science, 8(1): 1–17.
DOI: 10.3934/matersci.2021001
Received: 25 October 2020
Accepted: 28 December 2020
Published: 18 January 2021

http://www.aimspress.com/journal/Materials

Research article

Improving accuracy of surface roughness model while turning 9XC steel using a Titanium Nitride-coated cutting tool with Johnson and Box-Cox transformation

Vo Thi Nhu Uyen[1], and Nguyen Hong Son[2,*]

[1] Faculty of Mechanical Engineering, Hanoi University of Industry, Hanoi City, 100000, Vietnam
[2] Center for Mechanical Engineering, Hanoi University of Industry, Hanoi City, 100000, Vietnam

* **Correspondence:** Email: nguyenhongson@haui.edu.vn; Tel: +84945268696.

Abstract: The surface roughness model for predicting surface roughness during machining is built in order to deal with time constraints of adjusting and testing. This study aims to achieve this purpose. The 9XC steel turning experiment is performed on a CNC lathe with the cutting tool is Titanium Nitride-coated. The input parameters selected for the test matrix include cutting velocity, feed rate, depth of cut and tool nose radius. The experiments were carried out based on Central Composite Design (CCD) with 29 trials. The analysis of results using Minitab software reveals that feed rate is the most influential parameter, while the others have a negligible impact on surface roughness. The response surface method (RSM) is applied for modeling surface roughness. Johnson and Box-cox transformations are also used to develop two new models of surface roughness. The comparison of predicted results from these three models with experimental results shows that the Box-Cox-based model has the highest accuracy, followed by the Johnson while the model not using these transformation is the least. Mean absolute error and mean square error of the RSM-based model are 17.264% and 2.712% respectively; while they are 10.373% and 1.280% in the Johnson-based and 10.208% and 1.284% when using the Box-Cox transformation.

Keywords: 9XC steel; surface roughness model; Titanium Nitride-coated cutting tool; John transformation; Box-Cox transformation

Abbreviations: v_c: Cutting velocity; f: Feed rate; a_p: Depth of cut; r_ε: Tool nose radius; Ra: Surface roughness **(**Roughness average); RSM: Response surface method; MAE: Mean absolute error; MSE: Mean square error; CCD: Central composite design

1. Introduction

Turning is the most common of the cutting machining methods. Its workload accounts for 40% of the total machining and number of lathes makes up 25 to 35% of total machines in a cutting workshop [1]. Many factors affect the efficiency of the turning process such as surface roughness, dimensional accuracy, cutting force, cutting capacity, cutting heat, machining productivity, etc. And the surface roughness is significant to have an influence on the working ability and lifetime of the product and it is often chosen as a criterion to evaluate the efficiency of the turning process. Many studies were carried out to experiment with the effect of technological parameters on surface roughness when turning a workpiece with different materials.

The impacts of cutting velocity, feed rate and depth of cut on surface roughness during turning operation of AISI 4140 steel with a PVD-coated cutting tool were constructed [2]. This study indicated that the feed rate is the parameter that has the greatest influence on the surface roughness, followed by the cutting velocity, while depth of cut has a negligible effect.

Upon using coated carbide cutting tools for turning steel AISI 5140, the feed rate is the most influential parameter to surface roughness (accounting for 69.4%) in comparison with spindle speed and cutting edge angle [3]. When turning steel AISI 5140 by PVD coated carbide cutting tool, the feed rate is the most important parameter for surface roughness (accounting for 62.3%), followed by spindle speed, while depth of cut has nearly no effect on surface roughness [4].

When using coated carbide cutting tools for convenient steel AISI 5140, of the three parameters including cutting velocity, knife running and cutting edge angle, the amount of knife running is the most influential parameters to surface roughness (accounting for 69.4%) [3]. When conveniently steeling AISI 5140 with PVD coated carbide cutting tool, of three parameters including cutting velocity, knife run and cutting depth, knife running is the most influential parameters for surface roughness (accounting for 62.3%), followed by the impact of cutting velocity, while cutting depth has virtually no effect on surface roughness [4].

After implementing tests to find out how cutting velocity, feed rate, depth of cut and tool nose radius impact surface roughness using cutting tool coated with Al_2O_3 and TiC compounds for turning AISI 4140 steel, another study concluded: The feed rate and tool nose radius are the significant parameters [5].

The cutting velocity, feed rate and tool nose radius are found to importantly affect the surface roughness in turning process of EN 353 steel with the tungsten carbide-coated cutting tool, while the depth of cut are negligible [6]. Tests on the influence of cutting velocity, feed rate and depth of cut on surface roughness when turning titanium alloy TC11 with a carbide TiAlN coated cutting tool were implemented [7]. The feed rate is revealed to have the considerable impact on surface roughness, followed by cutting velocity. The depth of cut is fairly limited. When using the 41305A carbide cutting tool for turning 1Cr18Ni9Ti stainless steel, it was determined that the feed rate is the parameter that has the greatest effect on the surface roughness, followed by the cutting velocity while the depth of cut is not noticeable [8]. One study revealed that the cutting velocity and feed rate have a significant effect on the surface roughness and the depth of cut is negligible (for EN 8 steel and

CVD carbide cutting tool) [9]. In the test of turning Titanium-alloy workpiece with YG8 cutting tool (consisting of 92% tungsten carbide and 8% cobalt), the analysis results showed that influence of the feed rate on surface roughness was greater than the depth of cut and cutting velocity is the least among three cutting parameters [10]. When using the CNMG-type cutting piece for turning aluminum 6061, the input parameters to be considered include the tool nose radius, the feed rate and depth of cut. Their influence level to surface roughness is decreased correspondingly [11]. The effects of cutting velocity, feed rate and depth of cut on surface roughness when turning Inconel 718 material with carbide-coated tool was experimented [12]. The feed rate is the greatest-impacting parameter, followed by the cutting velocity, and the depth of cut that is the least. When turning AISI 4340 steel with a tungsten carbide-coated cutting tool under minimum quantity lubrication (MQL) conditions, four parameters including the cutting velocity, the feed rate, the depth of cut and the tool nose radius were considered. Only first three of them have a significant influence on surface roughness [13].

Among three cutting parameters of the input in the test of turning Ti–6Al–4V using cubic boron nitride (CBN) tool, the cutting velocity is the one that has the greatest effect on surface roughness, followed by depth of cut. The feed rate is not noticeable [14]. The impact of cutting velocity, feed rate and depth of cut on surface roughness when turning using carbide-coated tool was experimented [15]. This study showed that the feed rate and cutting velocity are two parameters that have great significance for surface roughness. But the depth of cut does not have importance to it. When using CNMG 12 04 08-PM 4225 cutting tool for turning AISI 1020 steel, the feed rate is main parameter to impact surface roughness, followed by depth of cut while cutting velocity is the least [16].

In the turning process of AISI 410 steel using ceramic-coated tool (supplied by Ceratizit), cutting velocity, feed rate and tool nose radius all have a significant effect on surface roughness. In which, the feed rate is the most influential parameter followed by the tool nose radius and cutting velocity. The depth of cut is negligible in this case [17]. The experiment using the CBN insert for dry turning EN 31 bearing steel indicates that the feed rate is the major impact. The cutting velocity also has a significant effect on the surface roughness, following the feed rate while the depth of cut is inconsiderable [18].

9XC is a high-alloy steel, commonly used to make components with tensile loads such as screws, bolts, shafts, gears; hot forging details; moving components or gear, connecting rod of pistons; parts with abrasion resistance, high impact resistance, rollers, etc. Table 1 shows its designation according to several standards.

Table 1. Designation of 9XC steel in several standards.

Country	Russian	USA	Britain	Britain	Japan	Germany
Standard	GOST	ASTM A29	EN 10250	BS 970	JIS G4103	DIN
Grades	9XC	4340	36CrNiMo4/1.6511	EN24/817M40	SNCM439/SNCM8	150Cr14

The research on surface roughness when turning some steel similar to 9XC is carried out by several studies. The operation of dry turning of EN24 steel using carbide cutting tool showed that all three cutting parameters including cutting velocity, feed rate and depth of cut have an influence on surface roughness: feed rate is the most considerable, followed by the cutting velocity while depth of cut has the limited impact on surface roughness [19]. When using multilayer CVD-coated

($TiN/TiCN/Al_2O_3$) carbide inserts for turning AISI 4340 steel, the effect of feed rate is significantly greater than the cutting velocity and depth of cut on surface roughness [20]. When using the PVCD-coated cutting tool for turning AISI 4340 steel, the cutting velocity and the feed rate have a considerable influence on the surface roughness. Increasing the cutting velocity reduces surface roughness. Decreasing the feed rate reduces it as well. Meanwhile, the depth of cut is insignificant to surface roughness [21].

The studies mentioned showed that cutting velocity, feed rate and depth of are often chosen as the input when conducting experimental research on the effect of these parameters on surface roughness during turning operation. The tool nose radius is also selected by some authors as the input parameter when researching the surface roughness of details during turning process. At the same time, the influence of cutting parameters on surface roughness is distinguished depending on the specific case of work piece and cutting tool material. It happens as well when turning steel which are similar to the 9XC. The authors of these studies also built surface roughness models using a method based on the relationship between surface roughness and cutting parameters and experimental research results. The method is called the response surface methodology (RSM).

Titanium Nitride-coated cutting tool has high hardness, high antioxidant properties. This type of cutting tool is widely used in metal machining [22,23]. However, number of research on the impact of cutting parameters on surface roughness in the turning process using this type of cutting piece to turn 9XC alloy steel (or equivalent) is fairly limited to date. Therefore, this study conducted experiments to determine the influence of cutting velocity, feed rate, depth of cut and tool nose radius on surface roughness when turning 9XC alloy steel with Titanium Nitride-coated cutting tool. The analysis of experimental results determined the influence of cutting velocity, feed rate, depth of cut and tool nose radius on the surface roughness. The RSM method is also applied for modeling surface roughness. In order to improve the model's accuracy for surface roughness prediction, Johnson and Box-Cox transformations were applied in this study. For each transformation used, a new model of surface roughness is proposed. Then, these models were assessed on the basis of their accuracy.

2. Experiment of turning 9XC steel

2.1. Material

The material used in the experiments is 9XC steel. Outer diameter and the sample length are 28 mm and 300 mm, respectively. The specimen is analyzed for spectrum and its chemical composition is introduced in Table 2. At a temperature of 20 ^oC, some basic features of this steel are presented in Table 3. Its specimens were heat-treated to reach a hardness of 52HRC.

Table 2. Chemical composition and properties of 9XC steel.

Element	C	Si	Mn	Ni	S	P	Cr	Mo	W	V	Ti	Cu
(%)	0.92	1.4	0.52	0.36	0.01	0.01	1.12	0.18	0.16	0.15	0.02	0.28

Table 3. Characteristics of 9XC steel.

Elastic modulus at 20 °C (GPa)	Elongation (%)	Poission's ratio	Tensile strength (MPa)	Yield strength (MPa)	Conefficient of thermal expansion (1/K)	Specific heat capacity (J/kg·K)	Thermal conductivity (W/m·K)
200–210	12	0.29	980	835	1.2×10^{-5}	450	44.5

2.2. Machine and cutting tool

The experiments are implemented using CNC Doosan Lynx 220L lathe. Tungsten cutting tool coated with Titanium nitride from Kyocera (Korea) is used. Tool nose radiuses are 0.2 mm, 0.4 mm, 0.6 mm, 0.8 mm and 1 mm. The five cuttin tools are labeled TNMG160402GP, TNMG160404GP, TNMG160406GP, TNMG160408GP and TNMG160410GP (Figure 1). Their rake angle, clearance angle, plane point angle, chip breaker angle are 7°, 5°, 75°, 7°, respectively. This type of cutting tool that has high hardness and temperature oxidation is commonly used in milling and turning so as to machine the workpiece with high hardness and heat resistance. Figure 2 presents some basic elements of the experimental system.

Figure 1. Cutting tools.

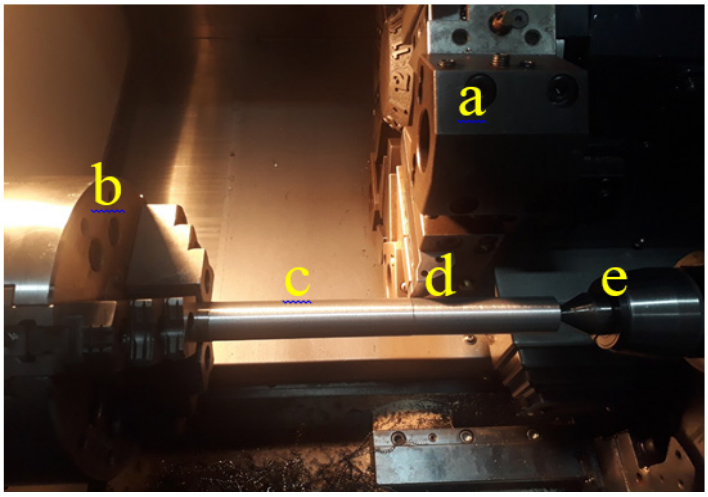

Figure 2. Basic elements of the experimental system. (a) Tool holder, (b) Three-jaw chuck, (c) Workpiece, (d) Cutting tool, and (e) Center.

2.3. Experiment plan

The experiments are intended to conduct based on the CCD. Each parameters is tested in 5 levels, including $-\alpha$, -1, 0, 1 and α. Where $\alpha = (2^k)^{1/4}$, k is the number of parameters. Four parameters selected as the input of the experiments includes cutting velocity, feed rate, depth of cut and tool nose radius. Their values can be changed by the operator simply. The values of each input at

all the levels are shown in Table 4. They are within the value range recommended by the manufacturer of the cutting tools. The test matrix includes 2^k of original points (at the levels of −1 and 1), 2 × k of axial points (at −α and α level) and 5 central points (at the level of 0) as shown in Table 5.

Table 4. Input parameters.

Parameter	Symbols	Unit	Value at levels				
			−2	−1	0	1	2
Cutting velocity	v_c	m/min	50	75	100	125	150
Feed rate	f	mm/rev	0.04	0.06	0.08	0.10	0.12
Depth of cut	a_p	mm	0.2	0.3	0.4	0.5	0.6
Tool nose radius	r	mm	0.2	0.4	0.6	0.8	1.0

Table 5. Test series matrix with code form of input parameters.

No.	v_c	f	a_p	r
1	1	−1	−1	1
2	0	0	−2	0
3	−2	0	0	0
4	−1	1	−1	−1
5	−1	1	−1	1
6	0	0	0	0
7	−1	−1	1	−1
8	1	−1	1	1
9	−1	−1	−1	−1
10	1	1	1	1
11	0	0	0	−2
12	−1	−1	1	1
13	−1	1	1	−1
14	1	1	1	−1
15	0	0	0	0
16	0	0	0	0
17	0	0	0	0
18	0	0	0	2
19	1	−1	−1	−1
20	1	−1	1	−1
21	1	1	−1	1
22	−1	−1	−1	1
23	−1	1	1	1
24	2	0	0	0
25	0	2	0	0
26	0	−2	0	0
27	1	1	−1	−1
28	0	0	2	0
29	0	0	0	0

2.4. Measuring instrument

Surface roughness measuring machine SJ-301 from Mytutoyo (Figure 3) was used to measure the roughness of the test specimens. Direction of the machine probe is parallel to the spindle of the workpiece (perpendicular to the direction of the cutting velocity vector). The standard length is 0.8 mm. Each specimen is measured at least three times. The roughness value of each test is the average of the successive measurements.

Figure 3. Surface roughness measuring machine SJ-301.

2.5. Machining condition

In addition to adjusting the value of the cutting parameters according to the matrix, cutting fluid is also used in the machining process. It is CN32 industrial oil (made in Vietnam) which has concentration of 10% and irrigation flow rate of 12 liters/min. To eliminate the effect of tool corrosion on surface roughness, each cutting tool is only used for one trial.

3. Result and discussion

The result is presented in Table 6. Figure 4 shows the impact of parameters on surface roughness. It indicated that the feed rate has the greatest influence on surface roughness and it is similar when using the carbide cutting tool to turn EN24 steel [19]. When the feed rate increases from 0.04 to 0.06 mm/rev, the surface roughness decreases. However, when the feed rate increases from 0.06 to 0.12 mm/rev, the surface roughness increases rapidly. While cutting velocity, depth of cut and tool nose radius have the negligible impact on the surface roughness.

Table 6. Experiment matrix and result.

No.	v_c (m/min)	f (mm/rev)	a_p (mm)	r (mm)	Ra (μm)
1	125	0.06	0.3	0.8	0.493
2	100	0.08	0.2	0.6	0.773
3	50	0.08	0.4	0.6	1.019
4	75	0.10	0.3	0.4	1.411
5	75	0.10	0.3	0.8	1.668
6	50	0.08	0.4	0.6	0.470
7	75	0.06	0.5	0.4	0.582
8	125	0.06	0.5	0.8	0.886
9	75	0.06	0.3	0.4	0.571
10	125	0.10	0.5	0.8	0.818
11	100	0.08	0.4	0.2	0.917
12	75	0.06	0.5	0.8	0.538
13	75	0.10	0.5	0.4	1.254
14	125	0.10	0.5	0.4	1.142
15	100	0.08	0.4	0.6	0.448
16	100	0.08	0.4	0.6	0.470
17	100	0.08	0.4	0.6	0.437
18	100	0.08	0.4	1.0	0.942
19	125	0.06	0.3	0.4	0.325
20	125	0.06	0.5	0.4	0.638
21	125	0.10	0.3	0.8	0.784
22	75	0.06	0.3	0.8	0.638
23	75	0.10	0.5	0.8	0.662
24	150	0.08	0.4	0.6	0.706
25	100	0.12	0.4	0.6	1.512
26	100	0.04	0.4	0.6	0.837
27	125	0.10	0.3	0.4	0.997
28	100	0.08	0.6	0.6	0.818
29	100	0.08	0.4	0.6	0.493

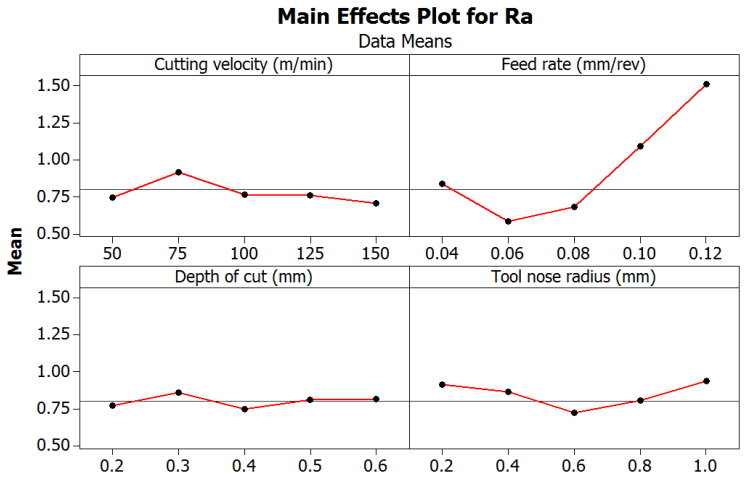

Figure 4. Main Effects Plot for surface roughness.

4. Surface roughness models

4.1. RSM-based model

Based on the experimental results in Table 6, a model of the relationship between surface roughness and parameters of the input is established, as shown in Eq 1. Building up the mathematical relationship between input and output is known as the response surface method (RSM) [24]. This model is the basis for choosing the value of the parameters to ensure that the surface roughness achieves the desired value. It is also used for predicting surface roughness after machining in each specific condition and in surveyed area. Figure 5 shows surface roughness results based on (1) and experiments.

$$Ra = 0.46360 - 0.07779 \times v_c + 0.22563 \times f - 0.01154 \times a_p - 0.01596 \times r_\varepsilon + 0.08263 \times v_c^2 + 0.16063 \times f^2 + 0.06588 \times a_p^2 + 0.09938 \times r_\varepsilon^2 + 0.09938 \times v_c \times f + 0.13356 \times v_c \times a_p + 0.01194 \times v_c \times r_\varepsilon - 0.10006 \times f \times a_p - 0.08194 \times f \times r_\varepsilon - 0.06194 \times a_p \times r_\varepsilon \quad (1)$$

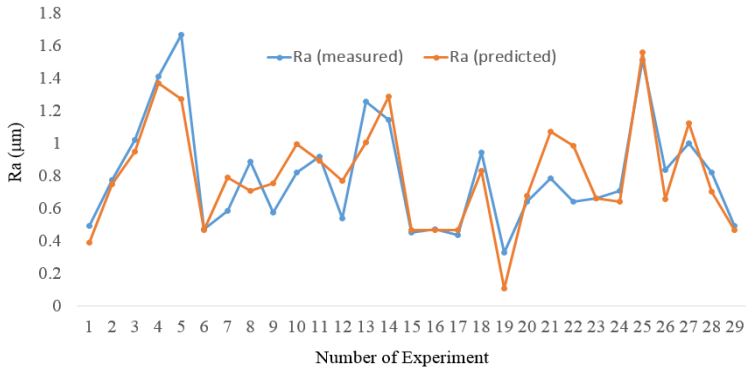

Figure 5. Surface roughness results based on experiments and (1).

Figure 5 shows that the surface roughness in prediction is considerably different with the results from many of 29 trials. The mean absolute error between the predicted and experimental results is 17.264%. It is necessary to develop surface roughness models so as to achieve higher accuracy in predicting surface roughness. Box-Cox and Johnson transformations are known as the techniques in order to improve the accuracy of the models [24]. This is the purpose for the authors to carry out the work in this study.

4.2. Probability plot of surface roughness

The study used Minitab 16 statistical software to determine the probability plot of surface roughness according to the data in Table 6 and the results are presented in Figure 6. The figure shows that the data were distributed fairly far from normal probability line. Moreover, the probability value P = 0.049 is smaller than the significance level (which is usually chosen as 0.05). Hence, it can be confirmed that the surface roughness values do not fit the normal distribution [24].

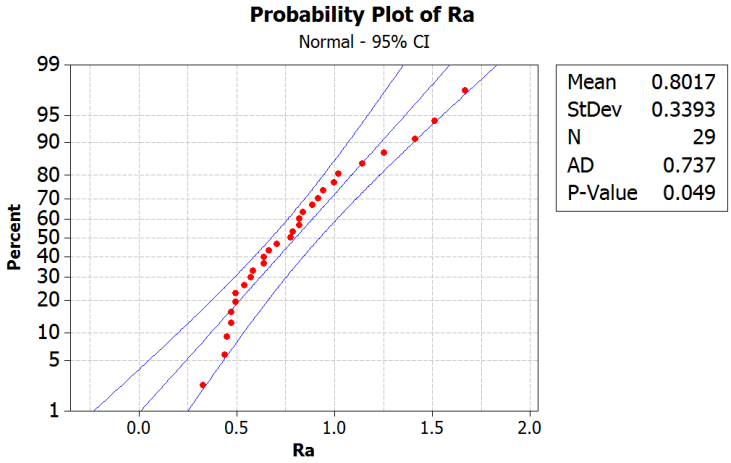

Figure 6. Probability plot of surface roughness.

4.3. Development of surface roughness with Johnson transformation

The Johnson transformation is used to convert a data set that does not follow the normal distribution pattern into a normal distribution [24,25]. The Minitab 16 statistical software was used to perform the Johnson transformation in order to convert the surface roughness data in Table 6. The results were presented in Figure 7 and Table 7.

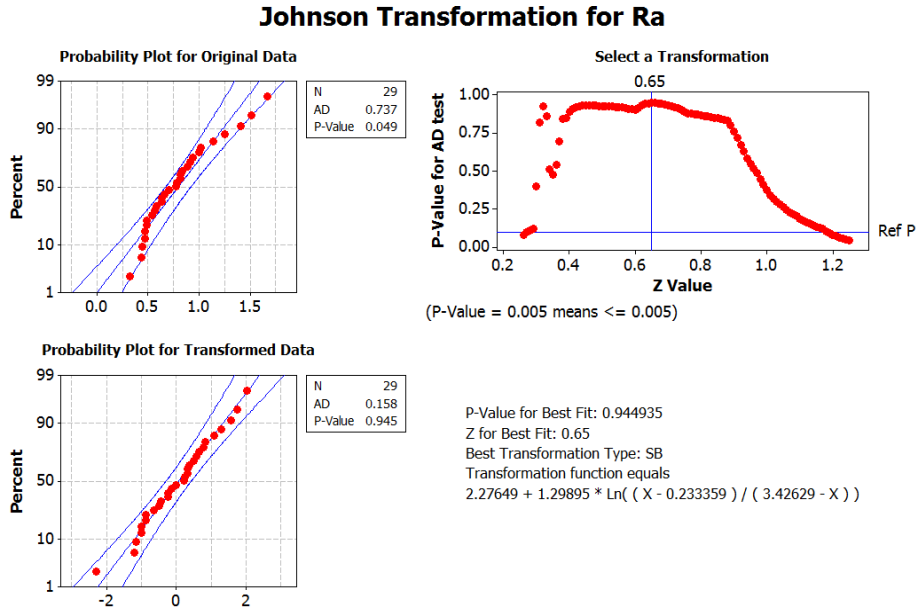

Figure 7. The Johnson transformation results for surface roughness.

The observation of the upper left area in Figure 7 showed that the data was distributed fairly far from the normal probability line (as analyzed in section probability plot of surface roughness), while the lower left off figure revealed that the data plot was close to normal probability line. In addtion, P value is 0.945 which was greater than the significance level. Thus, it can be said that the surface

roughness values fit the normal distribution. This proves that it is appropriate to apply Johnson tool for converting surface roughness data. The upper right section of the figure showed the data after Johnson transformation was distributed in the form of a curve. The lower right presented the relationship between the data after and before the Johnson conversion. As a result, the surface roughness model is shown in Eq 2.

$$2.27649 + 1.29895 \times \mathrm{Ln}((Ra–0.233359)/(3.42629−Ra)) = −1.04661 − 0.20923 \times v_c + 0.60895 \times f + 0.05401 \times a_p + 0.00299 \times r_\varepsilon + 0.29163 \times v_c^2 + 0.45566\times f^2 + 0.25620 \times a_p^2 + 0.34281 \times r_\varepsilon^2 − 0.07801 \times v_c \times f + 0.41624 \times v_c \times a_p + 0.11397 \times v_c \times r_\varepsilon − 0.32021 \times f \times a_p − 0.28270 \times f \times r_\varepsilon − 0.20182 \times a_p \times r_\varepsilon \quad (2)$$

Eq 2 is written as Eq 3.

$$Ra = (3.42629 \times \mathrm{Exp}(F) + 0.233359)/(\mathrm{Exp}(F) + 1) \quad (3)$$

In Eq 3, F is defined as the following Eq 4.

$$F = −2.55830 − 0.16107 \times v_c + 0.46881 \times f + 0.04158 \times a_p + 0.00230 \times r_\varepsilon + 0.22451 \times v_c^2 + 0.35079 \times f^2 + 0.19724 \times a_p^2 + 0.26391 \times r_\varepsilon^2 − 0.06006 \times v_c \times f + 0.32045 \times v_c \times a_p + 0.08774 \times v_c \times r_\varepsilon − 0.24652 \times f \times a_p − 0.21764 \times f \times r_\varepsilon − 0.15537 \times a_p \times r_\varepsilon \quad (4)$$

Table 7. Surface roughness before and after transformation.

Order	Surface roughness		
	Experiment (μm)	Johnson transformation (dimensionless)	Box-Cox transformation (dimensionless)
1	0.493	−0.873	−0.707
2	0.773	0.208	−0.257
3	1.019	0.822	0.019
4	1.411	1.579	0.344
5	1.668	2.012	0.512
6	0.47	−1.004	−0.755
7	0.582	−0.450	−0.541
8	0.886	0.511	−0.121
9	0.571	−0.497	−0.560
10	0.818	0.334	−0.201
11	0.917	0.587	−0.087
12	0.538	−0.645	−0.620
13	1.254	1.295	0.226
14	1.142	1.079	0.133
15	0.448	−1.140	−0.803
16	0.470	−1.004	−0.755
17	0.437	−1.213	−0.828
18	0.942	0.647	−0.060
19	0.325	−2.298	−1.124
20	0.638	−0.231	−0.449
21	0.784	0.239	−0.243
22	0.638	−0.231	−0.449
23	0.662	−0.145	−0.412
24	0.706	0.003	−0.348
25	1.512	1.752	0.413
26	0.837	0.385	−0.178
27	0.997	0.773	−0.003
28	0.818	0.334	−0.201
29	0.493	−0.873	−0.707

4.4. Development of surface roughness with Box-Cox transformation

The Box-Cox transformation is used to convert a data set that does not follow the normal distribution pattern into a normal distribution as well [24,26].

The transformation has the form:

$$\begin{cases} X' = X^{\lambda} \text{ when } \lambda \neq 0 \\ X' = \ln(X) \text{ when } \lambda = 0 \end{cases} \quad (5)$$

where X' is after-transformation data; X is before-transformation data; λ is the exponent of the transformation. The value λ is determined by detection, as long as the standard deviation of the converted data set is minimum. Box-Cox method performs the detection of λ in the range of −5 to 5, then round it to one of common values as shown in Table 8 [16,24].

Table 8. Common values of λ in Box-Cox transformation.

Value λ (dimensionless)	Transformation formula
$\lambda = 2$	$X' = X^2$
$\lambda = 0.5$	$X' = \sqrt{X}$
$\lambda = 0$	$X' = \ln X$
$\lambda = -0.5$	$X' = 1/\sqrt{X}$
$\lambda = -1$	$X' = 1/X$

Surface roughness data after the Box-Cox transformation was also included in Table 6. Figure 8 showed the distribution of surface roughness after the transformation. The plot was close to the normal probability line. And P value is 0.919 which was significant. Therefore, it can be seen that the surface roughness values follow the normal distribution. In other words, the Box-Cox transformation was also performed successfully in converting the non-normal-distributed data into the normal distribution.

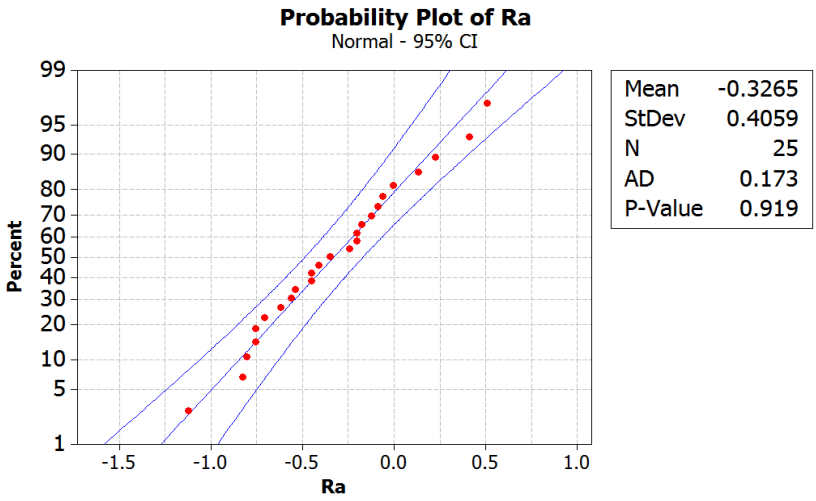

Figure 8. Probability plot of surface roughness after Box-Cox transformation.

Figure 8 showed a graph of the Box-Cox transformation function. From the results in this figure, the value of the exponent λ was determined to be zero. Thus, the surface roughness model after performing the Box-Cox transformation is defined as in Eq 6.

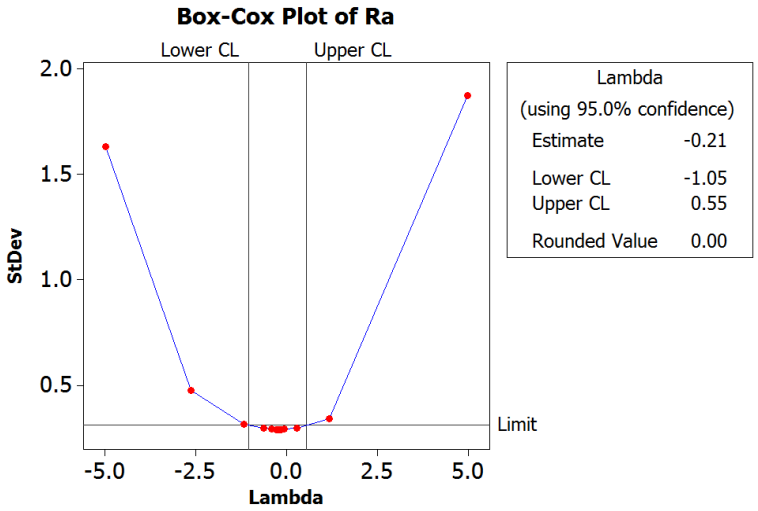

Figure 9. The Box-Cox transformation results for surface roughness.

$$\text{Ln(Ra)} = -0.76962 - 0.08120 \times v_c + 0.25461 \times f + 0.01494 \times a_p - 0.00893 \times r_\varepsilon + 0.12186 \times v_c^2 + 0.19247 \times f^2 + 0.10573 \times a_p^2 + 0.14473 \times r_\varepsilon^2 - 0.04710 \times v_c \times f + 0.16453 \times v_c \times a_p + 0.03814 \times v_c \times r_\varepsilon - 0.12332 \times f \times a_p - 0.11393 \times f \times r_\varepsilon - 0.07358 \times a_p \times r_\varepsilon \quad (6)$$

Eq 6 is written as Eq 7.

$$\text{Ra} = \text{Exp}(-0.76962 - 0.08120 \times v_c + 0.25461 \times f + 0.01494 \times a_p - 0.00893 \times r_\varepsilon + 0.12186 \times v_c^2 + 0.19247 \times f^2 + 0.10573 \times a_p^2 + 0.14473 \times r_\varepsilon^2 - 0.04710 \times v_c \times f + 0.16453 \times v_c \times a_p + 0.03814 \times v_c \times r_\varepsilon - 0.12332 \times f \times a_p - 0.11393 \times f \times r_\varepsilon - 0.07358 \times a_p \times r_\varepsilon) \quad (7)$$

To evaluate the accuracy of the three surface roughness models introduced (including the RSM, Johnson and Box-Cox-based), mean absolute error (MAE) and mean square error (MSE) of the predicted results and the experimental was compared. Values of MAE and MSE are defined as Eqs 8 and 9 below.

$$\%MAE = \left(\frac{1}{n}\sum_{i}^{n}\left|\frac{e_i - p_i}{e_i}\right|\right) * 100\% \quad (8)$$

$$\%MSE = \left(\frac{1}{n}\sum_{i}^{n}|e_i - p_i|^2\right) * 100\% \quad (9)$$

where e is experimental value; p is predicted value; n is a number of trials.

Table 9 presented the experimental and predicted value of surface roughness on the basis of RSM approach (Eq 1) and predicted surface roughness value on the basis of Johnson (Eqs 3 and 4) Box-cox (Eq 7) transformation.

Table 10 introduced comparison of the three models. The data revealed that: Compared with the model of the RSM method, the MAE decreased from 17.264% to 10.373%, the MSE decreased from 2.712% to 1.280% in the Johnson-based model, and the MAE decreased from 17.264% to 10.208%, the MSE decreased from 2.712% to 1.284% in the Box-Cox-based model. Deviation of MAE and MSE in the model using Box-Cox transformation was smaller than in the model using Johnson transformation. However, the difference is slight.

Table 9. Predicted surface roughness in models and Errors compared to experimental value.

Order	Experimental surface roughness Ra (μm)	Predicted surface roughness Ra (μm)			Absolute error (%) (Eq 8)			Square error (%) (Eq 9)		
		SRM (Eq 1)	Johnson (Eqs 3 and 4)	Box-Cox (Eq 7)	SRM	Johnson	Box-Cox	SRM	Johnson	Box-Cox
1	0.493	0.387	0.541	0.560	21.481	9.808	13.614	1.121	0.234	0.450
2	0.773	0.750	0.666	0.686	2.950	13.809	11.228	0.052	1.139	0.753
3	1.019	0.950	0.897	0.887	6.801	11.981	12.943	0.480	1.491	1.739
4	1.411	1.369	1.703	1.713	2.961	20.717	21.423	0.175	8.545	9.137
5	1.668	1.273	1.473	1.438	23.656	11.670	13.762	15.569	3.789	5.269
6	0.470	0.464	0.463	0.463	1.362	1.524	1.449	0.004	0.005	0.005
7	0.582	0.787	0.649	0.641	35.141	11.548	10.119	4.183	0.452	0.347
8	0.886	0.707	0.901	0.886	20.160	1.666	0.015	3.191	0.022	0.000
9	0.571	0.753	0.568	0.583	31.825	0.523	2.108	3.302	0.001	0.014
10	0.818	0.993	0.844	0.835	21.443	3.196	2.043	3.077	0.068	0.028
11	0.917	0.893	0.812	0.841	2.613	11.409	8.258	0.057	1.094	0.573
12	0.538	0.771	0.633	0.632	43.257	17.609	17.535	5.416	0.897	0.890
13	1.254	1.003	1.157	1.150	20.033	7.733	8.295	6.311	0.940	1.082
14	1.142	1.289	1.172	1.146	12.890	2.654	0.315	2.167	0.092	0.001
15	0.448	0.464	0.463	0.463	3.482	3.312	3.390	0.024	0.022	0.023
16	0.470	0.464	0.463	0.463	1.362	1.524	1.449	0.004	0.005	0.005
17	0.437	0.464	0.463	0.463	6.087	5.913	5.993	0.071	0.067	0.069
18	0.942	0.829	0.817	0.812	11.975	13.296	13.827	1.272	1.569	1.696
19	0.325	0.107	0.363	0.363	66.960	11.662	11.726	4.736	0.144	0.145
20	0.638	0.675	0.754	0.771	5.865	18.196	20.817	0.140	1.348	1.764
21	0.784	1.073	0.884	0.864	36.908	12.818	10.245	8.373	1.010	0.645
22	0.638	0.985	0.783	0.772	54.339	22.783	21.020	12.019	2.113	1.799
23	0.662	0.659	0.680	0.719	0.420	2.748	8.663	0.001	0.033	0.329
24	0.706	0.639	0.620	0.641	9.555	12.195	9.194	0.455	0.741	0.421
25	1.512	1.557	1.657	1.664	3.001	9.582	10.081	0.206	2.099	2.323
26	0.837	0.655	0.584	0.601	21.761	30.233	28.182	3.317	6.403	5.564
27	0.997	1.121	0.856	0.884	12.477	14.125	11.355	1.548	1.983	1.282
28	0.818	0.704	0.732	0.728	13.932	10.471	10.946	1.299	0.734	0.802
29	0.493	0.464	0.463	0.463	5.963	6.118	6.047	0.086	0.091	0.089

Table 10. Comparison between surface roughness models.

Models	% MAE	% MSE
With Johnson transformation	10.373	1.280
Box-Cox transformation	10.208	1.284
With RSM	17.264	2.712

5. Conclusion

In this study, the experiment of turning 9XC alloy steel using Titanium Nitride coated-cutting tools was conducted. The results identified the influence of input parameters on surface roughness. The study also proposed three models of surface roughness based on the experiments and Johnson and Box-Cox transformation. Some conclusions are drawn as follows:

-The feed rate is most influential to surface roughness. Other parameters including cutting velocity, depth of cut and tool nose radius have the negligible impact on the surface roughness.

-The surface roughness values from experiments does not fit the normal distribution. Johnson and Box-Cox transformation are used to convert the values in order to suit this distribution.

-Surface roughness model using Box-Cox transformation has the highest accuracy, followed by the Johnson-based while the model developed from testing results (without transformation) has the lowest accuracy.

-The comparison of results from three surface roughness models with experiments reveals that mean absolute error (MAE) of the model using the Box-Cox transformation, the Johnson-based and the RSM-based is 10.208%, 10.373% and 17.264%, respectively. In addition, the mean square error (MSE) value of the two models using the transformations is similar (1.284% and 1.280%) and noticeably smaller than the other's.

-The results obtained in this study show that the application of the Box-Cox and Johnson transformation is likely feasible in improving the accuracy of surface roughness models in particular and in developing regression models for machining methods in general.

Acknowledgments

Financial support from the Hanoi University of Industry for this research is acknowledged with gratitude.

Conflict of interest

There is no conflict of interests between authors.

References

1. Nguyen NT, Trung DD (2020) Modeling and improvement of the surface roughness model in hole turning process 3X13 stainless steel by Johnson transformation. *IJMPERD* 10: 12097–12110.
2. Zahia H, Athmane Y, Lakhdar B, et al. (2015) On the application of response surface methodology for predicting and optimizing surface roughness and cutting forces in hard turning by PVD coated insert. *IJIEC* 6: 267–284
3. Kuntoglu M, Aslan A, Pimenov DY, et al. (2020) Modeling of cutting parameters and tool geometry for multi-criteria optimization of surface roughness and vibration via response surface methodology in turning of AISI 5140 steel. *Materials* 13: 4242.

4. Kuntoglu M, Aslan A, Saglam H, et al. (2020) Optimization and analysis of surface roughness, flank wear and 5 different sensorial data via tool condition monitoring system in turning of AISI 5140. *Sensors* 20: 4377.
5. Meddour I, Yallese MA, Bensouilah H, et al. (2018) Prediction of surface roughness and cutting forces using RSM, ANN, and NSGA-II in finish turning of AISI 4140 hardened steel with mixed ceramic tool. *Int J Adv Manuf Tech* 97: 1931–1949.
6. Bhardwaj B, Kumar R, Singh PK (2013) Prediction of surface roughness in turning of EN 353 using response surface methodology. *T Indian I Metals* 67: 305–313.
7. Yang A, Han Y, Pan Y, et al. (2017) Optimum surface roughness prediction for titanium alloy by adopting response surface methodology. *Results Phys* 7: 1046–1050.
8. Xiao M, Shen X, Ma Y, et al. (2018) Prediction of surface roughness and optimization of cutting parameters of stainless steel turning based on RSM. *Math Probl Eng* 2018: 9051084.
9. Routara BC, Sahoo AK, Parida AK, et al. (2012) Response surface methodology and genetic algorithm used to optimize the cutting condition for surface roughness parameters in CNC turning. *Procedia Eng* 38: 1893–1904.
10. Yang C, Zheng Q, Hu Y (2016) The prediction model of surface roughness based on experiments of turning titanium alloy. *2016 IEEE International Conference on Mechatronics and Automation* 1776–1780.
11. Singh D, Chadha V, Singari RM (2016) Effect of nose radius on surface roughness during CNC turning using response surface methodology. *IJMECH* 5: 31–45.
12. Tebassi H, Yallese MA, Meddour I, et al. (2017) On the modeling of surface roughness and cutting force when turning of inconel 718 using artificial neural network and response surface methodology: Accuracy and benefit. *Period Polytech Mech Eng* 61: 1–11.
13. Patole PB, Kulkarni VV (2018) Prediction of surface roughness and cutting force under MQL turning of AISI 4340 with nano fluid by using response surface methodology. *Manuf Rev* 5: 5.
14. Sahu NK, Andhare AB, Andhale S, et al. (2018) Prediction of surface roughness in turning of Ti–6Al–4V using cutting parameters, forces and tool vibration. *IOP Conf Series Mater Sci Eng* 346: 012037.
15. Sahu NK, Andhare AB (2015) Optimization of surface roughness in turning of Ti–6Al–4V using response surface methodology and TLBO, *ASME 2015 International Design Engineering Technical Conferences and Computers and Information in Engineering Conference*, American Society of Mechanical Engineers, 4: V004T05A020.
16. Khidhir BA, Al-Oqaiel W, Kareem PM (2015) Prediction models by response surface methodology for turning operation. *Am J Model Optim* 3: 1–6.
17. Makadia AJ, Nanavati JI (2013) Optimisation of machining parameters for turning operationsbased on response surface methodology. *Measurement* 46: 1521–1529.
18. Karthik MS, Raju VR, Reddy KN, et al. (2020) Cutting parameters optimization for surface roughness during dry hard turning of EN 31 bearing steel using CBN insert. *Mater Today Proc* 26: 1119–1125.
19. Davis R, Madhukar JS, Rana VS, et al. (2012) Optimization of cutting parameters in dry turning operation of EN24 steel. *IJETAE* 2: 559–563.
20. Das SR, Nayak RP, Dhupal D, et al. (2014) Surface roughness, machining force and flank wear in turning of hardened AISI 4340 steel with coated carbide insert: Cutting parameters effects. *ASE* 4: 758–768.

21. Lima JG, Avila RF, Abrao AM, et al. (2005) Hard turning: AISI 4340 high strength low alloy steel and AISI D2 cold work tool steel. *J Mater Process Tech* 169: 388–395.
22. Klocke F, Krieg T (1999) Coated tools for metal cutting - features and applications. *CIRP Annals* 48: 515–525.
23. Prengel HG, Pfouts WR, Santhanam AT (1998) State of the art in hard coatings for carbide cutting tools. *Surf Coat Tech* 102: 183–190.
24. Dean A, Voss D, Draguljić D (2017) *Design and Analysis of Experiments Design of experiment techniques*, Springer.
25. Trung DD (2020) Influence of cutting parameters on surface roughness during milling AISI 1045 steel. *Tribol Ind* 42: 568–665.
26. Trung DD, Ngoc ND, Hong TT, et al. (2020) Influences of cutting parameters on surface roughness during milling and development of roughness model using Johnson transformation, In: Sattler KU, Nguyen DC, Vu NP, et al., *Advances in Engineering Research and Application*, *Lecture Notes in Networks and Systems*, Switzerland: Springer, Cham, 178: 491–450.

AIMS Press